

# DRIVING THE LHC COLLIMATORS' STEPPING MOTORS OVER 1 KM WITH HIGH ACCURACY AVOIDING EMI EFFECTS

A. Masi, G. Conte<sup>#</sup>, R. Losito, M. Martino, CERN, Geneva, Switzerland

## Abstract

The LHC collimators are exposed to very high levels of radiation, which means that the power drivers must be installed far from the stepping motors that they drive. Due to the geometry of the underground installations, the distances can be up to 1 km. The long cables that connect the drivers to the motors behave as transmission lines modifying dramatically the impedance seen by the drivers and consequently jeopardizing the control performance of Pulse Width Modulation (PWM) drivers. In this paper we address this problem, provide an analytical model of the driver-cable-motor system and describe the analog solution we have developed to improve the performance of a typical off the shelf driver. Finally we characterize the improvement of the performances with measurements of positioning repeatability and show that electromagnetic emissions from the long cables are drastically reduced, making the use of stepping motors compatible with extremely sensitive instrumentation such as the LHC Beam Loss Monitors (BLM).

## INTRODUCTION

Positioning the collimators in the Large Hadron Collider (LHC) is a critical task since collimators protect the LHC against uncontrolled beam losses [1]. Because of their excellent properties of repeatability, robustness and open loop positioning performance [2], radiation tolerant stepping motors have been chosen to move the 555 collimator axes with 5  $\mu\text{m}$  resolution. PWM (Pulse Width Modulation) drivers based on dynamic controllers or cheaper Hysteresis Current Regulators (HCR) are nowadays the most commonly used option to drive stepping motors, replacing traditional linear drivers mainly due to their higher efficiency [3]. Figure 1 shows the working principle of the PWM HCR drivers that power and control the LHC collimators' stepping motors.

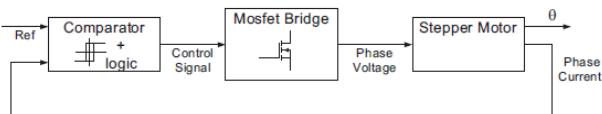


Figure 1: Working principle of the stepping motor driver SHS Star 2000 used for the LHC collimators.

An HCR performs nonlinear control of the motor phase currents by using feedback of measured currents. The control is performed with an analog comparator that computes the error between the measured value of the current and its reference. The MOSFET bridge, which generates PWM voltage signals, is controlled by the sign of the instantaneous current error.

In the radioactive environment of the LHC, commercial

electronic drivers cannot be located close to the stepping motors that they power but have to be installed in safe areas up to 1 km away. Despite this distance, they should guarantee the same positioning repeatability and low electromagnetic emissions not to interfere with other sensitive equipment.

At the typical PWM chopping frequencies of commercial stepping motor drivers (i.e. 20 kHz), long cables (hundreds of meters) behave as transmission lines [4], whose shunt capacitance significantly modify the current measured close to the driver for feedback with respect to the current that could be measured close to the motor. The former value is affected by a significant ringing effect, while the latter is in reality inaccessible during operation. Figure 2 compares the motor and driver side currents measured with a 280 meter long motor cable.

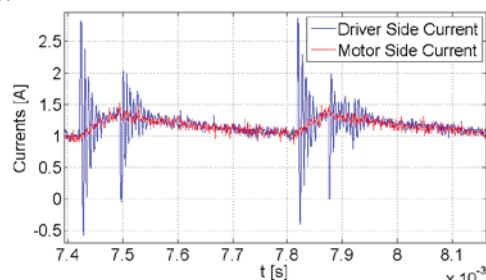


Figure 2: The ringing effect on the driver side current measured with a 280 meter long cable.

The error on the feedback current due to the ringing can cause serious consequences on the performance of the current controller [5]. On standard off-the-shelf HCR drivers, like those used for the LHC collimators, the control algorithm fails since the current used for feedback is directly sampled without any prior filtering. In this case it is necessary to wait for the decay of the ringing before closing the feedback loop on the measured current. This translates, for the cable lengths considered, to a drastic reduction of the PWM chopping frequency and results in huge motor phase current ripple (i.e. poor positioning repeatability) and radiated EMI emissions from the cable at low frequencies (i.e. a few kHz). These performances are not compatible with the demanding requirements of the stepping motor drivers of the LHC collimators [6].

In the following section the model of the driver-cable-stepping motor system, which was developed to study and characterize the problem, is presented. The solution found and implemented in LHC is then presented. A detailed experimental validation follows in the last section.

## MODEL OF A MOTOR WITH A CABLE

The model developed to understand and characterize the

ringing phenomenon on the driver side currents when a several hundred meter long cable is connected to a stepping motor is shown in Figure 3.

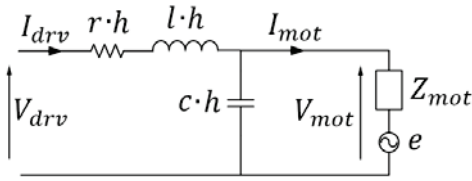


Figure 3: Equivalent electrical circuit of the cable and motor of the LHC collimators.

### Cable

The LHC motor cable is modelled as a transmission line. For a typical chopping frequency of 20 kHz significant spectral contents of the PWM signal driving the cable extend up to 90 kHz. In this frequency range a model with lump parameters with only one stage represents a good approximation of the transmission line [6].  $r$ ,  $l$  and  $c$  represent, respectively, the resistance, inductance and shunt capacitance per unit length and  $h$  is the cable length. In the frequency range of interest they are assumed constant and have the following values:  $r = 23 \Omega/\text{km}$ ,  $l = 0.6 \text{ mH}/\text{km}$  and  $c = 48.7 \text{ nF}/\text{km}$ .

### Motor

In Figure 3 the motor is represented by its equivalent Thevenin circuit with an impedance  $Z_{mot}(s)$  and the equivalent back electromotive force  $E(s)$ . A detailed motor model, including its iron losses, is shown in Figure 4.  $R_{fe}$  takes into account the real power dissipated by eddy currents and  $L_{fe}$  the reactive power stored by magnetic hysteresis. Both are functions of frequency and their analytical expressions have been evaluated by fitting experimental data [7].  $R_w$  and  $L_w$  represent the motor winding's resistance and inductance, respectively.

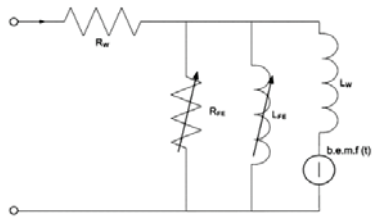


Figure 4: Equivalent motor phase circuit, including iron losses. b.e.m.f(t) is the back electromotive force.

The motors used, Maccon SM 87.2.18M2N, have the following electrical parameter values:  $R_w = 3.4 \Omega$ ,  $L_w = 30 \text{ mH}$ ,  $R_{fe} = 3040 \Omega$  and  $L_{fe} = 36.2 \text{ mH}$ . The  $R_{fe}$  and  $L_{fe}$  values have been evaluated at the PWM chopping frequency (i.e. 20 kHz).

From the detailed motor phase model in Figure 4,  $Z_{mot}(s)$  and  $E(s)$  in the equivalent motor circuit used in Figure 3 can be derived as:

$$Z_{mot}(s) = \frac{R_w + [L_{eq} + R_w \tau_{eq}]s}{1 + s\tau_{eq}} \approx \frac{R_w + L_{eq}s}{1 + s\tau_{eq}}, \quad (1)$$

where  $L_{eq} = L_w/L_{fe}$ ,  $\tau_{eq} = L_{eq}/R_{fe}$  and considering that  $L_{eq} + R_w \tau_{eq} = (1 + R_w/R_{fe})L_{eq} \approx L_{eq}$  since  $R_{fe} \gg R_w$ . Also:

$$E(s) = \frac{L_{fe} R_{fe}}{L_w L_{fe} s + R_{fe} L_w + L_{fe} R_{fe}} \text{ b.e.m.f}(s).$$

## THE PROPOSED SOLUTION

The driver-cable-motor system is modelled in Figure 5.

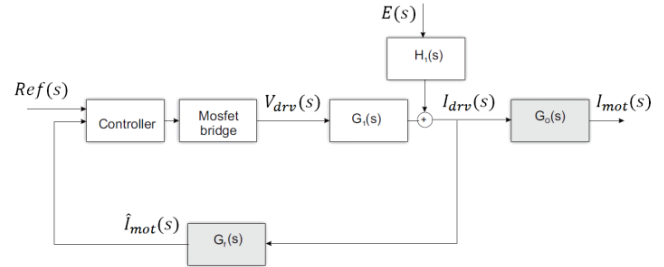


Figure 5: Block diagram of the entire system.

$I_{mot}(s)$  represents the motor side current,  $V_{drv}(s)$  the PWM control voltage supplied by the driver and  $I_{drv}(s)$  is the driver side current. Using the proposed model the transfer function  $G_o(s)$  from  $I_{drv}(s)$  to  $I_{mot}(s)$  can be evaluated by applying the current divider rule between the load impedance and the line capacitance to give:

$$G_o(s) = \frac{I_{mot}}{I_{drv}} = \frac{1}{1 + Z_{mot}(s)chs}. \quad (2)$$

It should be noted that a contribution from  $E(s)$  has been neglected in the above expression, but this can be considered negligible at standard stepping speeds [5].

### The Feedback Current Filter Design

The key principle of the proposed solution stays in the filtering strategy of the feedback current in order to remove the superimposed ringing error and thus make the long cable effectively transparent from the controller's point of view. The addition of the filter in the driver architecture is represented in Figure 5 by the transfer function  $G_f(s)$ . This block should provide the controller with an estimate of the motor side current,  $\hat{I}_{mot}(s)$ , using only the driver side current as its input. The filter's transfer function is therefore that of  $G_o(s)$  in (2). Using (1) in (2),  $G_f(s)$  can be written as follows:

$$G_f(s) = \frac{1 + s\tau_{eq}}{1 + \tau_{eq}s + L_{eq}chs^2},$$

which also assumes  $\tau_{eq} + R_w ch \approx \tau_{eq}$  since  $\tau_{eq} \gg R_w ch$ .

### The Filter Implementation

An analog implementation of the filter was necessary to be compatible with the driver design (i.e. analog HCR). Fig. 6 shows a circuit implementing a transfer function with one zero and two complex poles since:

$$G(s) = \frac{V_o}{V_{IN}} = \frac{1 + sR_2C_2}{1 + sR_2C_2 + C_1C_2R_1R_2s^2}.$$

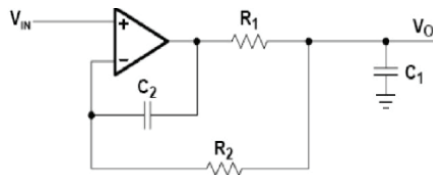


Figure 6: Analog implementation of the de-ringing filter.

Setting  $R_2 C_2 = \tau_{eq}$ , since  $\tau_{eq} = L_{eq}/R_{fc}$  is fixed once the chopping frequency is chosen, and  $C_1 C_2 R_1 R_2 = L_{eq} ch$  we have that  $R_1 C_1 = R_{fc} ch$ . Thus, if  $C_1$  is fixed, the resistance  $R_1$  can be tuned based on the cable length.

## THE EXPERIMENTAL VALIDATION

All experiments use an 800m cable, unless specified.

### The Filter's Estimation Performance

Figure 7 compares the true motor side current with the estimated one, calculated by  $G_f(s)$  using the driver side current shown. It can be seen that the true and estimated signals are very similar. It also demonstrates the need for the filter since very poor current regulation is obtained when the drive side current is directly used for feedback.

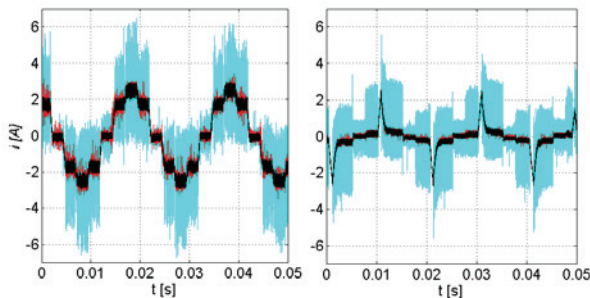


Figure 7: Current waveforms ( $I_{drv}$  (blue),  $\hat{I}_{mot}$  (red),  $I_{mot}$  (black)) achieved when  $G_f(s)$ 's output is used for feedback (left) and when  $I_{drv}$  is directly fed back (right).

### The Positioning Repeatability

Figure 8 shows the histograms of the motor's steady state position after a half step of  $0.9^\circ$ . The performance achieved when the estimated motor side current is used for feedback and when the drive side current is directly fed back is shown. The significant improvement obtained using the filtered current, in terms of the reduced position variance, can be clearly seen from the very different values of standard deviation,  $\sigma = 0.14^\circ$  vs.  $\sigma = 0.50^\circ$ . The former value is a typical tolerance given by manufacturers in the case of a motor driven with a very short cable.

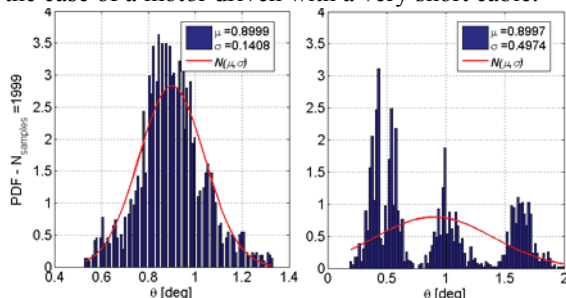


Figure 8: Comparison of the positioning histograms achieved with (left) and without (right) the filter  $G_f(s)$ .

## Electromagnetic Emissions

The EM emissions of the drive have been measured. Whilst being comparable to the emissions of the drive without a cable, see Figure 9, it was desirable to reduce the emissions further. This was achieved using a toroidal choke EMI filter with an inductance of 8.4 mH, chosen through extensive experimental testing. While the EMI filter negligibly affects the system's differential inductance, it significantly increases the common mode inductance and, as is clear from Figure 9, reduces radiated emissions, especially when the motor is running.

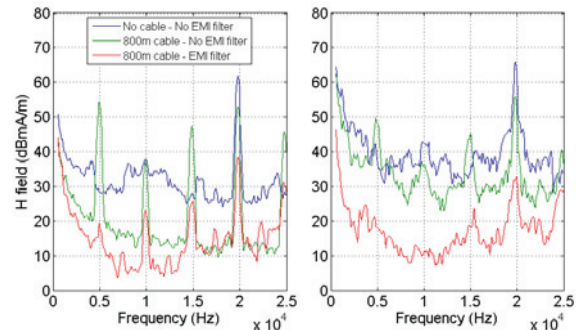


Figure 9: Comparison of emissions in holding (left) and running (right) with and without EMI filter and cable.

## CONCLUSIONS

The problems of using PWM HCR stepping motor drivers with long cables have been presented. A solution has been proposed and experimentally validated by application to the drivers used to power and control the stepping motors of the LHC collimators.

## REFERENCES

- [1] R. Assmann et al., "The final collimation system for the LHC", EPAC 2006, Edinburgh, U.K., 2006.
- [2] A. Masi and R. Losito, "LHC Collimators low level control system," *IEEE Trans. on Nucl. Sci.*, vol. 55, no. 1, pp.333-340, Feb. 2008.
- [3] T. Kenjo and A. Sugawara, "Stepping Motors and their Microprocessor Controls", 2nd ed., Oxford Univ. Press, Oxford, UK, 1994.
- [4] R.J. Kerkman, D. Leggate and G.L. Skibinski, "Interaction of drive modulation and cable parameters on AC motor transients," *IEEE Trans. on Industry Applications*, vol.33, no.3, pp.722-731, May/June 1997.
- [5] M. Martino, A. Masi, R. Losito and R. Picatoste Ruilope, "Low emission, self-tunable DSP based Stepping Motor Driver for use with arbitrarily long cables", 12th IFAC Symposium on Large Scale Systems: Theory and Applications, 2010.
- [6] G. Conte, "Control optimization of the LHC collimators stepping motor drivers", M.S. thesis, 2006.
- [7] A. Masi, G. Conte, R. Losito and M. Martino, "DSP-Based Stepping Motor Drivers for the LHC Collimators," *IEEE Trans. on Nucl. Sci.*, vol.55, no.1, pp.341-348, Feb. 2008.